PNAS RESEARCH ARTICLE | APPLIED BIOLOGICAL SCIENCES ENVIRONMENTAL SCIENCES
OPEN ACCESS

Shifting drivers and predictable corridors of an illegal wildlife trade network

George Olah[a,b,1], Rodrigo León-Pérez[c], Alex J. Berryman[d], Gregory P. Asner[e], and Robert Heinsohn[a]

Affiliations are included on p. 8.

Edited by Gerardo Ceballos, Universidad Nacional Autonoma de Mexico, Ciudad de México, Mexico; received March 15, 2026; accepted June 5, 2026

Illegal wildlife trade is a major driver of biodiversity loss but the lack of understanding of mechanisms sustaining criminal networks hampers law enforcement. We integrated three decades of confiscation data, criminological modeling, and spatial network analysis to dissect the illegal parrot trade in Mexico, a global hotspot of parrot diversity and endemism. Our interdisciplinary approach revealed that the wildlife trade is the leading threat, elevating their extinction risk. Trade is shifting from poverty-driven to population density-linked patterns. Circuit theory-based landscape modeling identified critical trade routes from biodiverse habitats to urban centers, providing actionable targets for law enforcement. Our study demonstrates the effectiveness of combining criminological methods with landscape science to identify specific trafficking routes, a transferable framework for generating actionable intelligence. Crucially, because illicit wildlife networks frequently converge with broader organized crime, this spatial framework provides a powerful proxy for exposing the shared logistical corridors of global illicit markets.

wildlife trafficking | circuit theory | conservation criminology | socioeconomic drivers | parrot trade

Significance

Criminal networks driving the multibillion-dollar illegal wildlife trade are notoriously difficult to map, forcing law enforcement into a reactive posture. We address this by pioneering an interdisciplinary framework, repurposing circuit theory from landscape ecology to make these hidden networks visible. Applying our model to three decades of data from Mexico's parrot trade, we reveal the trade's "hidden highways" and show how the network's drivers have fundamentally evolved from rural poverty to urban demand. This predictive approach provides a transferable roadmap for authorities to proactively dismantle not only wildlife trafficking but other illicit supply chains, offering a data-driven tool to protect global biodiversity and enhance security.

Illegal wildlife trade comprises global, multibillion-dollar criminal enterprises that threaten biodiversity and elevate the risk of zoonotic disease transfer and emergence (1–3). Despite its scale and impact, efforts to combat trafficking are usually reactive. Criminal networks are complex, adaptive, and largely invisible, making them notoriously difficult to map, track, and disrupt (4). A new approach is needed to move from enforcement-based, isolated seizures to a predictive understanding of network structure and vulnerability.

Parrots (Psittaciformes) are among the world's most heavily traded taxa, and Mexico is a global hotspot for their diversity and a focal point of their trafficking (5, 6). The Mexican parrot trade provides an excellent natural experiment to study trafficking dynamics. Over the past three decades, the network has been subjected to a series of major shocks: the cessation of legal exports to the United States in 1992 (7) and the EU in 2007, a complete national ban on capture and trade in 2008 (8), and the global disruption caused by the COVID-19 pandemic in 2020, which imposed severe restrictions on human mobility and shifted law enforcement priorities away from environmental protection (9). This sequence of distinct periods offers an exceptional opportunity to dissect how a complex trafficking network adapts to shifting pressures and enforcement regimes.

Here, by integrating three decades of confiscation data (from 1997 to 2024; *SI Appendix*, Table S1) with criminological theory and landscape-based circuit modeling, we identify the evolution of this network. By applying these frameworks longitudinally rather than as a static snapshot, we reveal a fundamental shift in the trade's socioeconomic drivers over time. By mapping the flow of trafficked birds, we pinpoint the critical corridors that form the network's backbone. Our analysis provides a transferable framework for generating actionable intelligence, offering authorities tools for proactively identifying the dynamics of criminal enterprises that threaten wildlife.

Trapping for the Wildlife Trade Elevates Extinction Risk

Half of Mexico's native parrot species are directly threatened by trapping for the illegal wildlife trade (*SI Appendix*, Table S2), a pressure that is elevating their risk of extinction. The overall conservation status for the country's parrots has deteriorated over the past three decades, with our analysis of IUCN Red List data and the Red List Index (RLI) showing a consistent deterioration across species with none showing improvement since 1993 (Fig. 1*A*). While the Mexican RLI for all bird species is above 0.9, Mexican parrots are tracking below 0.7 underscoring an already severe state of endangerment for this group. The apparent stabilization of the index in recent years likely reflects the broad nature of

Author contributions: G.O. and R.H. designed research; G.O. and R.L.-P. performed research; G.O., A.J.B., and G.P.A. contributed new analytic tools; G.O. and A.J.B. analyzed data; and G.O., R.L.-P., A.J.B., G.P.A., and R.H. wrote the paper.

The authors declare no competing interest.

This article is a PNAS Direct Submission.

[1]To whom correspondence may be addressed. Email: george.olah@anu.edu.au.

This article contains supporting information online at https://www.pnas.org/lookup/suppl/doi:10.1073/pnas.2609240123/-/DCSupplemental.

Published August 24, 2026.

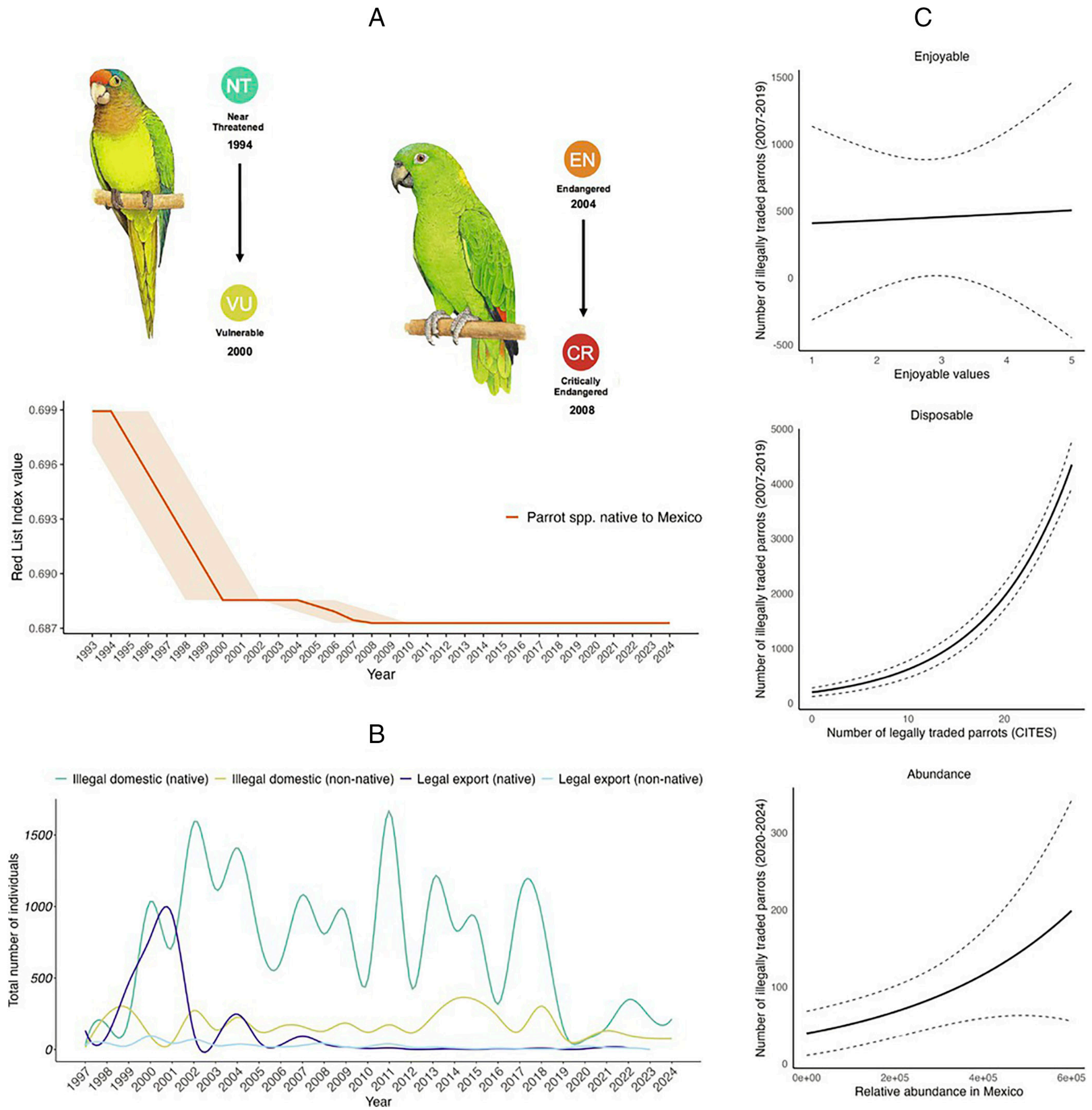

Fig. 1. The escalating crisis and shifting drivers of the Mexican parrot trade. (*A*) Deteriorating conservation status of Mexican parrots, shown by the Red List Index (RLI) from 1993 to 2024. A value of 1 indicates all species are Least Concern and 0 indicates Extinct. The shaded area represents the 95% CI. *Insets* show the species (*Eupsittula canicularis* on *Left* and *Amazona auropalliata* on *Right*) whose IUCN Red List status deteriorated (i.e. increased in extinction risk) during this period, driving the decline seen in the RLI. The stable plateau in recent years likely reflects the broad nature of the Red List categories, which renders the RLI relatively insensitive to minor changes in population or distribution parameters, as well as the periodicity of formal IUCN assessments and the inherent time lag in detecting wild population declines, rather than a true demographic stabilization. Illustrations [by Àngels Jutglar and Norman Arlott] courtesy of Cornell Lab of Ornithology, from Birds of the World (https://doi.org/10.2173/bow). (*B*) Trends in trade volume, showing the total number of individuals traded annually from 1997 to 2024. The illegal trade is based on domestic confiscation data, while the legal trade on CITES export data. Native and nonnative species to Mexico are plotted separately. (*C*) Drivers of species selection. Predicted effects from the best-fit CRAAVED models show that trade volume is significantly driven by how "enjoyable" (aesthetic appeal) and "disposable" (export potential) a species is (2009–2019), and by its local "abundance" (2020–2024). Solid lines are predicted values; dashed lines are 95% CI.

the Red List categories which renders the RLI relatively insensitive to minor changes in population or distribution parameters, as well as the well-documented time lag between genuine population deteriorations occurring on the ground (i.e., increases in extinction risk), their detection in field data, and subsequent formal IUCN reassessments (10). While habitat loss from agricultural expansion (affecting 45% of species) and logging (35%) are significant pressures, our analysis of IUCN threat classifications shows that illegal trapping is the most prevalent (50%) and highest-impact threat driving this decline (*SI Appendix*, Fig. S1).

Crucially, these threats do not act in isolation. Our network analysis reveals that trapping, agriculture, and logging form a tightly clustered overlap of threats, meaning they frequently co-occur and create synergistic pressures on the same species (*SI Appendix*, Fig. S2).

The edges of deforested areas, for example, enable easier access for poaching activities that often coexist with logging (11). This shows that parrot conservation needs a focus that addresses both habitat loss (12) together with an understanding of the drivers of illegal trade.

Dynamics of a Vast and Selective Trade Network

Analysis of over 6,000 confiscation records (1997–2024) reveals a vast illegal trade that has affected every native parrot species in Mexico (*SI Appendix*, Table S1). To understand its development, we examined the trade across three periods defined by the major policy shifts outlined above: bans on imports to USA and EU, 1997–2008; national ban on capture and trade, 2009–2019; and global disruption caused by COVID-19, 2020–2024. While confiscation volumes peaked in 2011 (1,668 individuals over all native species) and have declined since 2019 (Fig. 1*B*), the underlying trade has remained dynamic, with its geographic hotspots shifting over time from southern and coastal states toward a greater concentration in and around major urban centers (Fig. 2 and *SI Appendix*, Table S3).

Importantly, poachers consistently targeted a core group of large, charismatic, and high-value species, particularly macaws

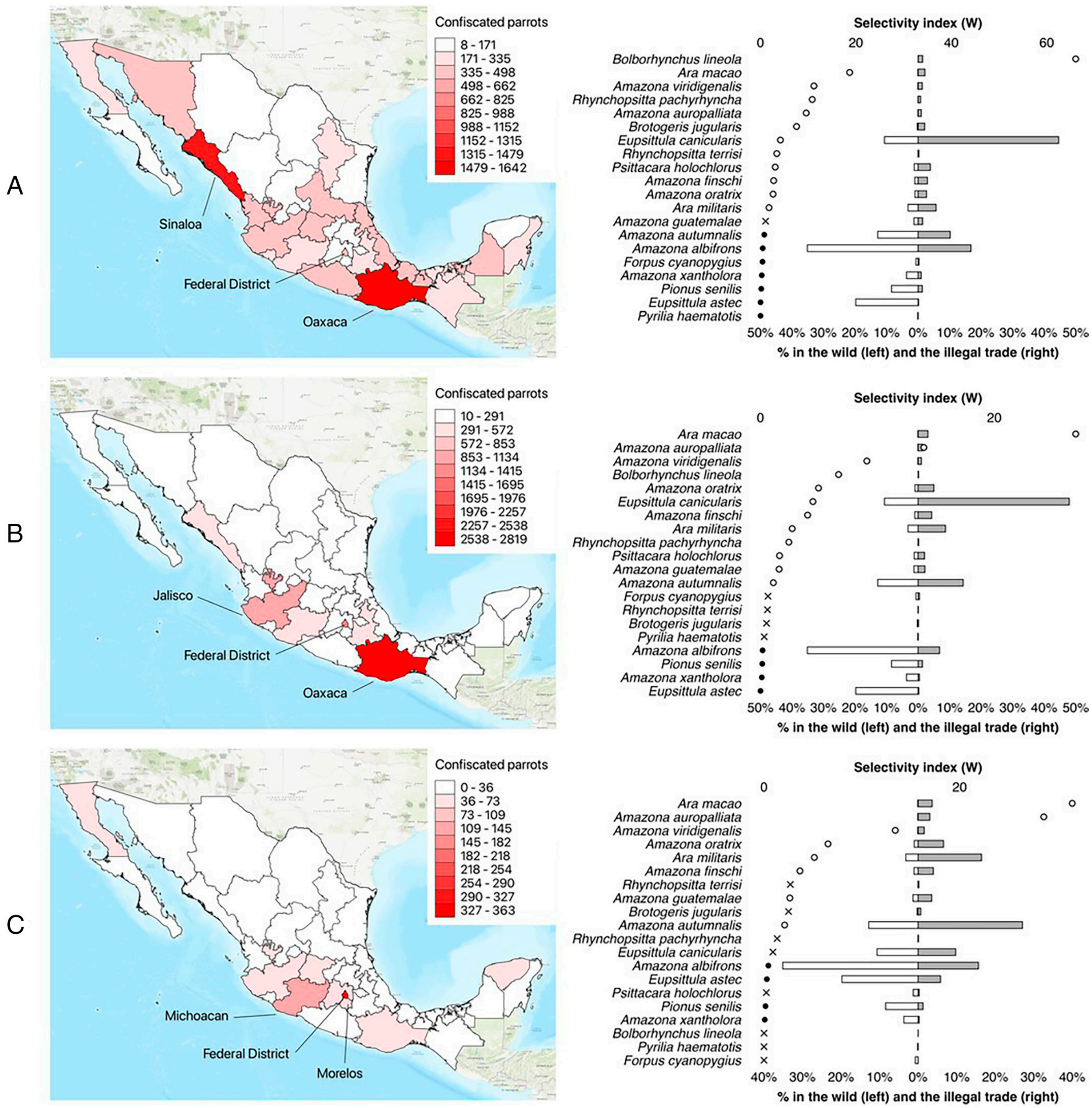

Fig. 2. Spatiotemporal patterns of parrot confiscations and trade selectivity. Maps show the total number of confiscated parrots by Mexican state for the periods 1997–2008 (*A*), 2009–2019 (*B*), and 2020–2024 (*C*). For each period, the corresponding charts on the right show species selectivity. Within the charts, white bars represent relative abundance in the wild, and dark gray bars show the proportion found in the illegal trade. Symbols indicate the Savage selectivity index (W) result: significant positive selection (empty circle), nonsignificant selection (cross), and significant negative selection (black circle). Species are listed in descending order of their selectivity index.

(*Ara* spp.) and Amazon parrots (*Amazona* spp.), at rates considered unsustainable compared to their natural abundance across all three periods (Fig. 2). While this core demand for iconic species has been also observed in other countries (13) and remained stable in Mexico, selection for smaller or less-colorful species fluctuated (Fig. 2), suggesting a two-tiered trade structure with both consistent and opportunistic components.

A key pattern emerged from these data. For many commonly traded species, confiscations occurred hundreds of kilometers from their native habitats, frequently in major cities like Mexico City (Fig. 2). This persistent geographic disconnect between source and seizure is indicative of an organized, long-distance trafficking network. These dynamics, the shifting hotspots, the stable high-value core, and the long-distance transport, necessitate a specific approach to identify the drivers and hidden routes that sustain the trade.

The Trade's Evolution from Poverty-driven to Urban Demand

The drivers of Mexico's illegal parrot trade have fundamentally shifted over the past three decades, evolving from a trade of opportunity rooted in rural poverty to demand centered on urban population density. To uncover these drivers, we analyzed the trade across three time periods using two parallel approaches: socioeconomic models to link the trade to state-level indicators, and criminological modeling to distinguish between opportunity and demand-driven trafficking (*Materials and Methods*).

Our analysis reveals a clear change in the factors driving the trade. In the pre-ban era (1997–2008), trade was significantly correlated with state-level poverty indicators (*SI Appendix*, Table S4). The selection of species was only weakly linked to their availability on the legal export market ("disposable"; *SI Appendix*, Table S5*A*), suggesting a trade largely driven by local, opportunistic poaching for supplemental income (14, 15).

After the 2008 national ban, the network's drivers transformed. The trade remained linked to poverty but also became strongly associated with human population size (*SI Appendix*, Table S4). Concurrently, species selection became powerfully driven by demand: traffickers targeted species that are more attractive and desirable as pets ("enjoyable"; Fig. 1*C* and *SI Appendix*, Table S5*B*), and easier to export ("disposable"; Fig. 1*C*). While the visual trend is moderate for "enjoyable" (Fig. 1*C*) due to the high variance inherent in seizure data, the model confirms a consistent positive relationship (*SI Appendix*, Table S5*B*). This indicates a shift toward a more organized trade catering to specific consumer preferences in growing urban areas. This finding is congruent with Tella and Hiraldo (16), who found that attractiveness was an important factor in the legal trade of parrots in Mexico. Similar results have also been found in the illegal parrot trade in Indonesia (17).

By the most recent period (2020–2024), the socioeconomic link to poverty had vanished and been replaced by human population size as the sole significant driver, cementing the role of urban centers as the nexus of demand (*SI Appendix*, Table S4). Correspondingly, the motivation for species selection shifted again. Instead of

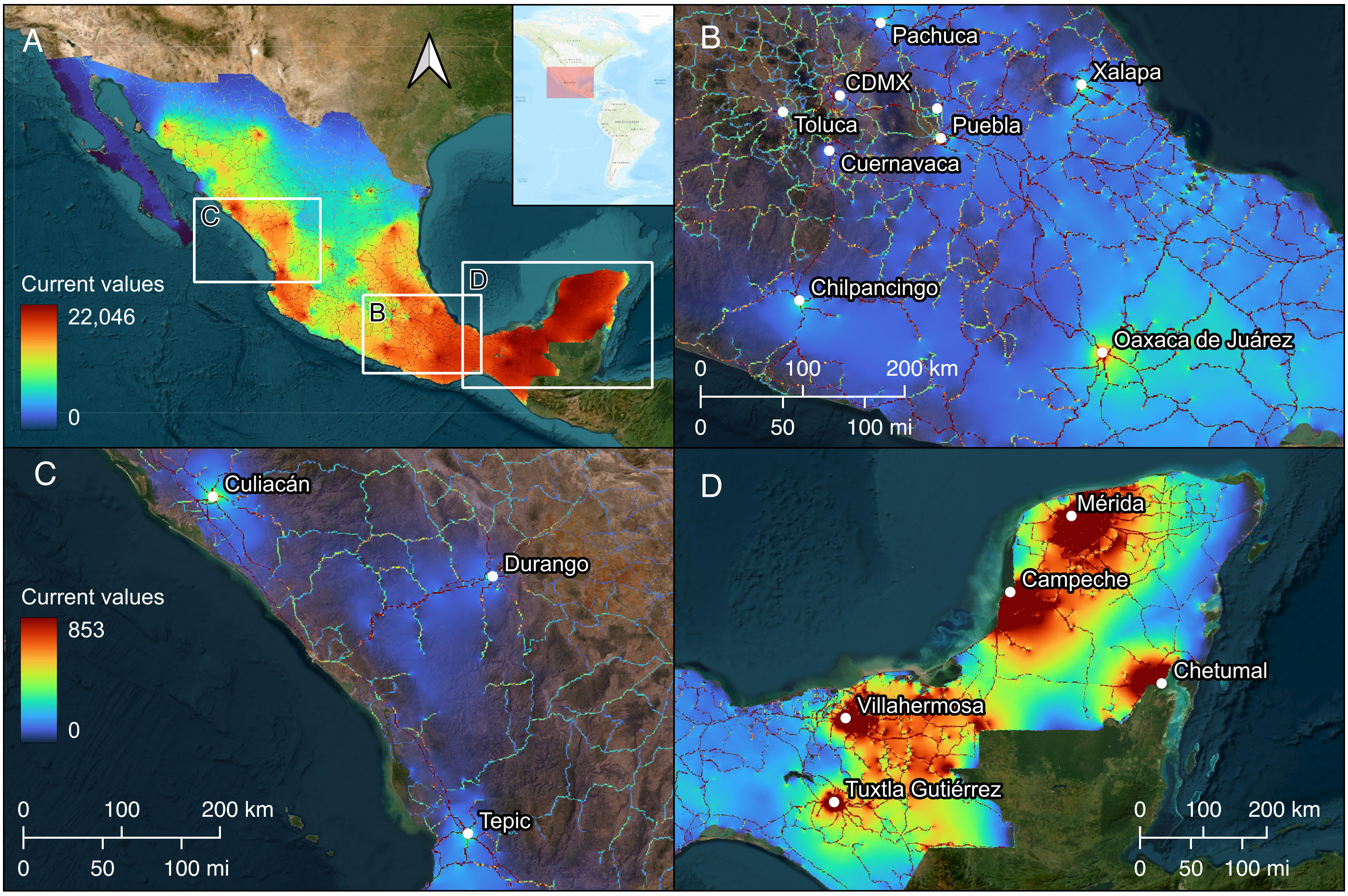

Fig. 3. Predicted corridors of the illegal parrot trafficking network in Mexico. (*A*) Cumulative predicted current map from the circuit theory analysis, highlighting the roads most likely used for illegal parrot trade. Hotspots are shown for central (*B*), western (*C*), and southeastern (*D*) Mexico, with warmer colors indicating higher predicted trafficking flow. Note that the current values for *B*–*D* are shown in the legend of *C*. Maps were created using QGIS v3.3 with ESRI Satellite (ArcGIS/World_Imagery) as basemap.

targeting species for their specific desirability ("enjoyable"), the trade became driven primarily by "abundance" (Fig. 1*C* and *SI Appendix*, Table S5*B*), suggesting a new, opportunistic strategy emerging to supply the large urban market with the most readily available species.

Mapping the Corridors of the Trafficking Network

The fundamental shift from a poverty-driven, opportunistic trade to one catering to urban demand with a new sourcing strategy implies a reorganization of the trafficking network itself. To visualize this network and identify the critical corridors connecting supply to demand, we applied spatial circuit theory.

Building on our understanding of the trade's evolving drivers, we mapped the physical pathways of the trafficking network. We adapted circuit theory, a tool used to model ecological connectivity (18, 19), to map illicit trade routes. We modeled the entire country as an electrical grid where parrots "flowed" from their source habitats to the urban areas where they are seized by authorities. By treating the road network as the conductive wire, the model calculates the "current" to reveal the flow intensity of trafficking across Mexico (*Materials and Methods*).

The analysis produced a nationwide map of the trade's hidden highways (Fig. 3*A*). Rather than being diffuse, the model revealed that trafficking is concentrated along specific, high-current corridors. The highest concentration of trafficking flow occurs in southeastern Mexico, comprising a network of critical routes in the areas east of the Isthmus of Tehuantepec and across the Yucatan Peninsula (Fig. 3*D*). Key roads leading to or through the cities of Villahermosa, Tuxtla Gutiérrez, Mérida, and Campeche showed the most intense activities. Other significant corridors were identified in southern Mexico converging on Oaxaca de Juárez (Fig. 3*B*) and along the Pacific slopes of western Mexico (Fig. 3*C*).

This map provides strategic insights useful in the fight against wildlife crime. Although Fig. 3 presents a static overview, we have translated these results into a secure, interactive online tool, accessible to verified law enforcement officials via a restricted portal (https://www.stopparrottrade.org) (20). It allows officials to zoom into their specific jurisdictions, inspect high-risk routes in detail, and filter the map by individual species (see Fig. 4 as an example for the case of the Military Macaw) to focus monitoring and interdiction efforts. This interactive system delivers the actionable intelligence proposed by our framework, creating a truly dynamic and intelligence-led platform for proactive enforcement. While the model's precision is naturally limited by the resolution of available seizure data, it provides a comprehensive data-driven roadmap of an entire country's illegal trade network for a broad taxonomic group. Furthermore, even though our application focused on road networks—the primary conduit for the domestic parrot trade (13)—the framework is flexible: by modifying the landscape resistance surface, future applications can easily incorporate multimodal transport routes, such as maritime shipping lanes or clandestine flight corridors.

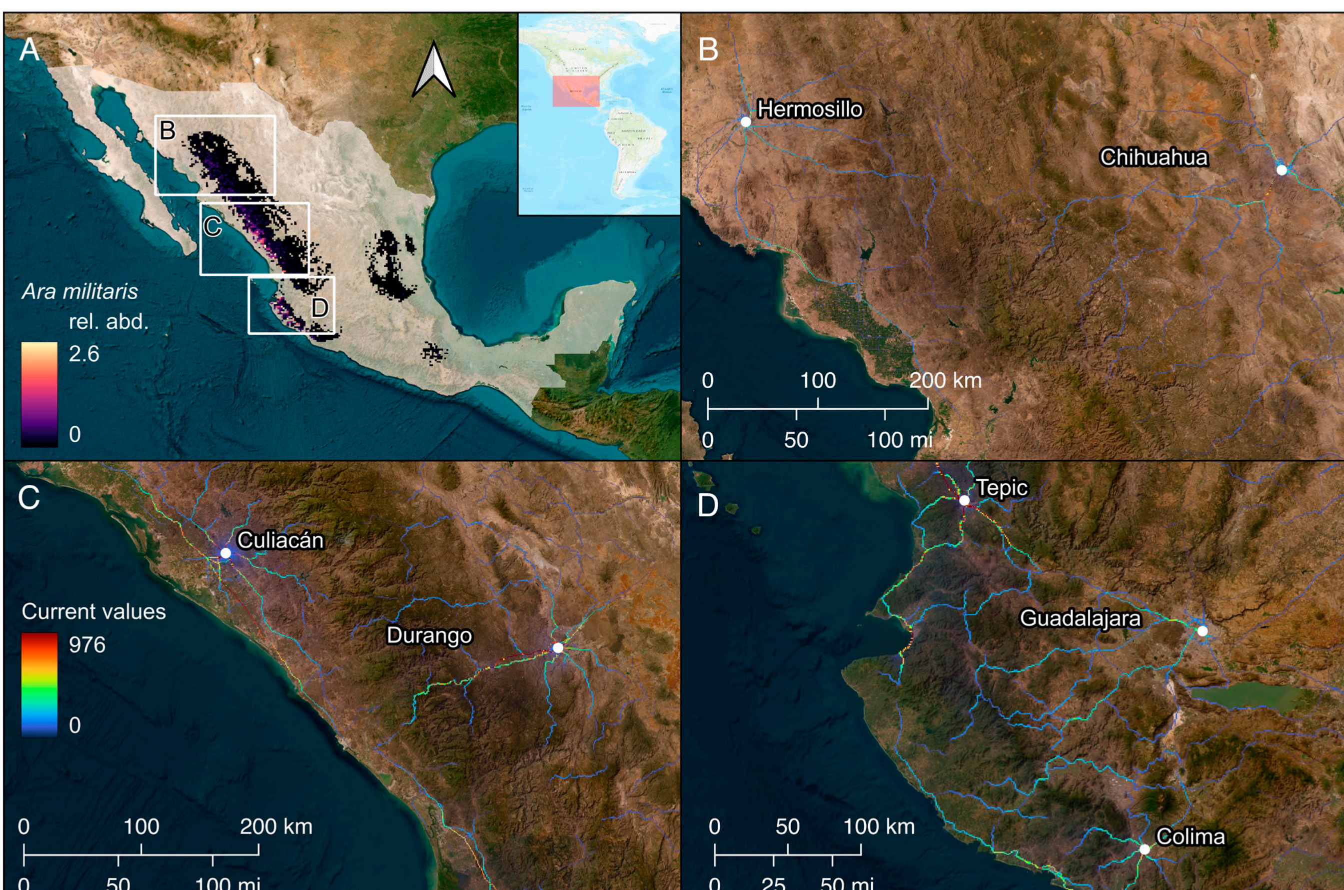

Fig. 4. Trade model for a single species, the Military Macaw (*Ara militaris*). (*A*) Relative abundance (rel. abd.) map of the Military Macaw in Mexico. (*B*–*D*) Predicted trade routes (current maps) from its natural range to confiscation locations, showing an overview of northwestern (*B*) and western Mexico (*C*), with a detailed view of the high-current area around Jalisco state (*D*). Maps were created using QGIS v3.3 with ESRI Satellite (ArcGIS/World_Imagery) as basemap.

Conclusions

By integrating criminological theory with landscape-scale network modeling, we have made a complex and illicit trade network visible and predictable. This can help move law enforcement efforts against wildlife crime from a reactive posture, dependent on isolated seizures, to a proactive one capable of identifying and anticipating the dynamics of these criminal enterprises, allowing interventions where they may be most effective. Our finding that the trade's drivers evolve, from poverty-based opportunism to urban-centered demand, provides a robust framework for designing conservation policies that can adapt to changing socioeconomic landscapes (21).

The implications of this interdisciplinary approach extend far beyond parrot conservation in Mexico. The "source-to-sink" circuit theory framework is a transferable paradigm that can be adapted to map other complex illicit networks, such as the trafficking of timber (22), marine life (23), or even drugs and weapons (24). Crucially, these illicit markets do not operate in isolation. There is a high degree of convergence between wildlife trafficking and broader organized crime (25). For example, drug cartels in Mexico regularly run illegal logging operations, sharing transport logistics and laundering illicit timber alongside narcotics (26). Similarly, transnational drug syndicates are increasingly comingling profits and utilizing shared smuggling infrastructure to traffic high-value wildlife (25). Because multifaceted crime groups exploit the same established paid corridors for combined contraband (25), mapping the domestic routes of a high-volume wildlife commodity like parrots provides a powerful proxy for exposing the hidden logistical architecture of more heavily guarded illicit supply chains.

In monitoring the wildlife trade, a key future direction is to enhance the precision of these models by establishing DNA reference databases for the most traded species (27). Currently, there is no standardized database available for parrots, and the lack of validated DNA reference sequences is hindering our ability to accurately assign provenance of confiscated birds over a large-scale (27). Establishing DNA reference databases for the most traded parrot species would be essential for forensic caseworks and to aid rewilding projects. The power of fusing landscape resistance modeling with genomic data has recently been demonstrated in reconstructing complex, live parrot trade networks operated by pre-Hispanic cultures across the Andes (28). Applying this integrated approach to modern law enforcement with forensic genetics would allow not only for the tracking of routes but also for the strengthening of legal cases and the targeted reinforcement of source populations (29). By revealing the hidden architecture of these enterprises, such data-driven approaches provide a new arsenal of tools to protect global biodiversity and enhance security.

Materials and Methods

Background of Parrot Trade in Mexico. The parrot trade in Mexico has a deep and long cultural history. Many Neotropical parrot species are known to have been popular in pre-Columbian cultures across South America (28, 30) to the North American Southwest (31) and traded up to 2,000 years ago (32). In the present, the confusion and complexity of changing laws (sometimes banning, sometimes permitting domestic trade) have contributed to ongoing illegal trade, in part because of the persistence of traditional practices and differing perceptions of legality (33).

Mexico has 20 native parrot species (*SI Appendix*, Table S1)—or 22 species following AviList v2025 (*Dataset Construction*)—that are mainly distributed along the Pacific coast north to the Sierra Madre Occidental, the coast of the Mexican Bay north to the Sierra Madre Oriental, and the Yucatan Peninsula. Some alien populations of native species were introduced by humans to the Valley of Mexico. Many of the native species are Amazon parrots (eight *Amazona* spp.) but also include two species of macaws (*Ara* spp.), three species of the previously recognized genus *Aratinga* (two *Eupsittula* spp. and one *Psittacara* sp.), two *Rhynchopsitta* spp. specialized in montane pine forests, and five other species of parrots, parakeets, and parrotlets (of the genera *Bolborhynchus*, *Brotogeris*, *Forpus*, *Pionus*, and *Pyrilia*).

In the 1970s and 1980s, many thousands of parrots were exported internationally, mainly to the United States until that country's importation of wild birds was halted by the Wild Bird Conservation Act (7). However, Mexico's parrot trade continued with tens of thousands of parrots captured and traded domestically with many still exported (14). The Federal Attorney for Environmental Protection (PROFEPA hereafter) was established in 1992, which has kept records of confiscations regularly since 1997. Export of parrots was further reduced when the European Union implemented an import ban on live birds in 2005 to prevent the spread of avian influenza (H5N1), which was made permanent in 2007. In October 2008, Mexico enacted a prohibition on the capture, trade, export, import, and captive breeding of parrot species native to the country (8). In 2020, a global pandemic was declared due to COVID-19, which halted many domestic operations in Mexico, including the activities of PROFEPA to prevent and monitor the wildlife trade.

RLI and Threats. The RLI is an indicator that shows trends in extinction risk for groups of species over time and is now widely used by governments to track their progress toward targets for reducing biodiversity loss (34). It is calculated using IUCN Red List data and changes between categories driven by genuine changes to extinction risk, and excludes changes caused by improved knowledge or revisions to taxonomy. The number of species in each IUCN Red List category in each year is multiplied by "equal step" scores (Least Concern, Near Threatened, Vulnerable, Endangered, Critically Endangered, and Extinct are scored from 0 to 5, respectively) and expressed as a fraction of the maximum sum (where all species have gone extinct) (35, 36). To calculate a national RLI for Mexican parrots, we followed Rodrigues et al. (37) and disaggregated the global RLI (1994–2024) and weighted each parrot species by the proportion of its range in Mexico (i.e., we calculated Mexico's contribution to global parrot extinction). CI (95%) for both values were derived following Butchart et al. (38).

We used a dataset from BirdLife International containing threat information for birds, where threats are classified according to the IUCN Threats Classification Scheme 3.3. Level 1 threats include broad categories (e.g., "Agriculture & aquaculture"), while Level 2 refines these into more specific subcategories (e.g., "Annual & perennial non-timber crops" or "Livestock farming & ranching"). The impact scores were calculated by BirdLife International from timing, scope, and severity for each threat by species where relevant. We used the second-level threats and their scores indicating low (scores 3 to 5), medium (6 to 7), and high impact (8 to 9). To assess the prevalence of these threats, we calculated the percentage of parrot species native to Mexico affected by each threat category. We constructed a heatmap using the "ggplot2" package of R (39) to compare threat categories across species, with threat intensity based on the average impact score per species. To explore interactions between co-occurring threats, we conducted a network analysis where edges represented shared threats among species. We visualized the network using the "ggraph" package of R (40).

Dataset Construction. To investigate the illegal aspect of the parrot trade, we requested access to the dataset on confiscated parrots in Mexico from PROFEPA via the National Institute for Transparency, Access to Information and Protection of Personal Data (INAI; access #PFPA/1.3/12C.6/2663/2024) since 1997 until 2024 (41). To study the legal aspect of the trade, we consulted the CITES trade database (https://trade.cites.org). We extracted the number of live parrot specimens of any Psittaciformes exported from Mexico to any countries between 1997 and 2024.

To better understand trends over time, we divided the confiscation data into three periods of (A) 1997–2008, (B) 2009–2019, and (C) 2020–2024. Most of the time-sensitive variables, including "concealable", "accessible", "valuable", and "disposable", were also calculated separately for each of these time periods (see details below).

We followed the taxonomy of HBW and BirdLife Taxonomic Checklist v10 (42) in all acquired datasets for comparability. Thus, we treat Pacific Parakeet *Psittacara* [*holochlorus*] *strenuus* and Socorro Parakeet *Psittacara* [*holochlorus*] *brevipes* as subspecies of Green Parakeet *Psittacara holochlorus*. We acknowledge that AviList v2025 (43) treats these two taxa as species but separating them in our study would have been problematic for the retrospective nature of our analysis and the lack of their Red List conservation status. The Monk Parakeet *Myiopsitta monachus* is introduced to Mexico and was excluded from analysis.

CRAAVED Models with Phylogenetic Control. The criminological model CRAAVED (standing for "concealable", "removable", "accessible", and "abundant" as opportunity-based factors, and "valuable", "enjoyable", and "disposable" as demand-side components) was developed to study the theft variation and drivers behind the wildlife trade (15, 44). This was applied to the parrot trade in Mexico first as a case study, and based on poaching estimates through interviews up until 2005, it found that widely abundant, easily poached species were the main target of the trade (15). Based on the same data, another study showed a selective capture of more attractive and valuable species (16). Since these studies, confiscation data on parrots have been systematically collected at the state level in Mexico, providing an opportunity to conduct more in-depth analyses and reveal trends over the past three decades.

For the CRAAVED models, we constructed a dataset of 20 parrot species native to Mexico. For each species, we assigned the seven CRAAVED components (15, 45), and calculated variance inflation factor (VIF) values for all explanatory variables with the "car" package in R (46), which measures multicollinearity among predictors, where higher values indicate stronger collinearity. All variables had VIF values < 5.

To determine if a species is "concealable", i.e., legal trapping is not possible and the species is harder to conceal from law enforcement, we used the version of the Mexican Official Standard NOM-059-SEMARNAT-2010 (which addresses the conservation status of native flora and fauna in Mexico) that was in force during the corresponding time period of A (47), B (47), and C (48). From the national red list, we recoded the categories ordinally as "1" for none protected status, "2" for "subject to special protection" (Pr), "3" for "threatened" (A), and "4" for "in danger of extinction" (P).

We inferred how "removable" each species is from the wild, by collecting information on their nest locations from published reference sources (49, 50). We categorized each species as "1" for reasonably easy (hollows in palm trees, where ladders might be used to access the nest), "2" for medium (cavities in hardwood trees and their branches, where rope access knowledge is required), or "3" for difficult (hollows in dead trees, arboreal termite mounds, or cliff walls, where access can be very challenging and/or dangerous).

We evaluated how "accessible" parrot species are to humans by overlapping species range distributions with human population density data. We extracted range distribution polygons for the 20 focus species (51), excluding polygons where the species is categorized as extinct but including all other instances (extant and possibly extant, native, and introduced origin). We acquired spatial distribution of human population density for Mexico in 2000 for time period A, 2010 for B, and 2020 for C as raster format with approximately 1-km-resolution (52). We overlapped each species distribution polygon with the human population raster data and calculated the total number of people living within each species' range by zonal statistics in QGIS 3.34 (https://www.qgis.org).

To estimate the "abundance" of each parrot species in Mexico, we first downloaded raster layers containing the year-round mean relative abundance data for each study species from eBird (https://science.ebird.org). We utilized the eBird Status data because they employ a machine learning modeling framework that can control for observer bias and generate estimates in unsampled sites (53). By using these methods to model the relationship between abundance and environmental covariates, robust abundance estimation is possible even in regions where direct observer coverage is limited. Relative abundance is defined as the estimated average count of individuals detected by an eBirder during a 1-h, 2-km traveling checklist at the optimal time of day for each species. Since eBird maps represent relative abundance per pixel, not total bird counts, we summed them for relative comparisons across states and the total area of Mexico, acknowledging that they do not represent true population sizes. Relative abundance data were not available for *Rhynchopsitta pachyrhyncha*, so we used data from *Rhynchopsitta terrisi* which has similar abundance.

We used the IUCN RedList categorization as a proxy whereby more threatened species are more "valuable" (16, 17, 54). We used values from 2006, 2019, and 2024 (55) for the time periods A, B, and C, respectively. We followed other studies by converting the categories into ordinal values ("1" = Least Concern, "2" = Near Threatened, "3" = Vulnerable, "4" = Endangered, "5" = Critically Endangered) (5, 56, 57).

We measured if a species is "enjoyable", i.e., attractive as a pet to potential customers, as a sum of the following four factors: color richness, color brightness, ability to mimic human speech, and size. We used data of a previously published study (58) that measured the percentage of body covered by different, human-visible colors for almost all bird species. For color richness, we first counted the number of 18 color categories (*SI Appendix*, Fig. S3) that in average between males and females covered at least 1% of their body, then assigned the value of "2" if more than the group's average number of colors were recorded, and "1" if otherwise. For color brightness, we first summed the percentage of body covered by brightly colored feathers (blue, purple, red, saturated green, and saturated yellow), and then assigned "1" if more than the group's average percentage of the body was brightly colored, and "0" if otherwise. These data were not available for *Amazona auropalliata* and *Amazona oratrix*, so we used measures from the similar *Amazona ochrocephala* instead. Species that had a good ability to mimic human speech in captivity, were assigned the value of "1", otherwise "0", based on a published study (59). Size of the species (from the top of the head to the end of the tail) was extracted from Forshaw (50), and the value of "1" was assigned to species that were larger than the group's average, and "0" if otherwise. The sum of these four values resulted in a score of "1" to "5" (where "5" = most attractive).

We expected that species that are exported in higher numbers are more "disposable", i.e., they can be sold more easily in illicit or licit markets. Using the data acquired from the CITES trade database, we calculated the total number of live individuals of each native parrot species of Mexico exported internationally for the corresponding time periods.

We used the total number of confiscated individuals of the parrot species native to Mexico between 1997 and 2024 and log-transformed it as our response variable. We standardized all explanatory variables with Z-score normalization that centers each variable around a mean of "0" and scales it to a SD of "1", ensuring they contribute equally to the model. First, we fitted a logistic regression model using the "GLM" function in R statistics (60) to calculate *P*-values for the seven explanatory variables. Then, we compared the Akaike information criterion (AIC) of all combinations of the seven variables without interactions and selected the best model with the lowest AIC using the "MuMIn" package in R (61). We repeated these steps for each time period. Since some of the species were not confiscated during one or more periods, in these models we introduced a small constant of "0.001" before log-transforming the response variable.

To control for phylogenetic relatedness, we used phylogenetic trees of the 20 parrot species native to Mexico (62). Since these trees are generated with pseudoposterior distributions (63), to account for potential uncertainties in the branch lengths and nodes separating species, we downloaded 1,000 possible phylogenetic trees of these species from the birdtree.org dataset (Ericson stage 2 backbone). For each of the 1,000 phylogenies, we performed a phylogenetic generalized linear mixed model (PGLMM) using the "pglmm_compare" function of the "phyr" R package (64, 65). The explanatory and response variables were the same as those used in the logistic regression model. For each explanatory variable, we report the average estimates of the regression coefficients (B), z-scores for the fixed effects regression coefficients (Z), and the *P*-values, accounting for phylogenetic relatedness. For each model, we report the average random effects variances for nested random effects (s2) with SD. We also report the coefficient of determination of each model (R^2_{pred}), computed from the variance between observed and predicted values, with the "rr2" R package (66).

We acknowledge that confiscation data may be biased toward larger, vocal species that are easier for law enforcement to detect. However, by log-transforming the response variable and explicitly including size as component of the "enjoyable" variable, our model accounts for the influence of these traits. Furthermore, because species-specific detectability remains constant over time, the observed shifts in significant drivers across the three decades reflect genuine changes in trade dynamics rather than detection artifacts.

Selectivity Index. In order to evaluate if parrot species are poached proportionally to their abundance in the wild, we calculated the Savage selectivity index (W) with modifications established for the parrot trade (67, 68). Briefly, we first divided the proportion of a given species recorded on the illegal trade (confiscation dataset) by the proportion of the relative abundance of the same species in the wild ("abundance" data described above). We tested the null hypothesis that parrot species are poached in proportion to their availability in the wild by comparing the statistics of "W" to the corresponding critical value of the chi-squared distribution after Bonferroni correction, with one degree of freedom (68). We repeated these steps for the three time periods.

Sociodemographic GLM Models. To test whether certain sociodemographic indicators (including human marginalization, human population size, education, and poverty) explain the illegal parrot trade among different states in Mexico, we conducted logistic regressions. For each time period, we fitted a logistic regression model using the GLM function in R statistics (60) to calculate *P*-values for each explanatory variable separately, in single terms. For the response variable, we used the number of confiscated parrots (per state per time period).

For the explanatory variables, we acquired 11 standard sociodemographic indicators defined by the National Institute of Statistics and Geography of Mexico (INEGI; https://en.www.inegi.org.mx/datosabiertos). We used the Mexican Marginalization Index (IM) developed by the National Population Council (CONAPO; https://datos.gob.mx/busca/dataset/indice-de-marginacion-carencias-poblacionales-por-localidad-municipio-y-entidad) that measures social disadvantages across states, and 10 standard national indicators that it is based upon (*SI Appendix*, Table S4). We acquired these data by each state for three decades (the years 2000, 2010, and 2020) corresponding to our three time periods.

Spatial Network Analysis. For the spatial analysis, we downloaded polygon shapefiles for the 32 states of Mexico (69) and aligned these with the Mexican confiscation datasets. The Federal District was renamed to Mexico City in 2016, and we will use its new name in the text. We visualized the data in QGIS 3.34 (https://www.qgis.org) by time period and parrot species to evaluate trends.

To analyze potential trade routes at a more granular level, we used spatial network analysis in CIRCUITSCAPE v5 (70), with relative abundance data on species in the wild and trade data on the states where they were confiscated. CIRCUITSCAPE uses electrical circuit theory to model connectivity across landscapes (18). We used its "advanced" mode in Julia v1.11.2 environment (https://julialang.org) to simulate "flows" of wildlife trade from source areas (wild populations) to grounds (confiscation points) across resistance surfaces representing potential trade routes.

For current source maps, we used the eBird's relative abundance maps (excluding R. pachyrhyncha without spatial data; see above). Each raster cell value (the relative abundance) specified the source strength in the model. For the ground points, we generated individual raster layers for each species based on their confiscation data in each state, assigning the values of confiscated individuals to a single raster cell where the capital city of a given states is found, as exact confiscation locations within the states were unknown. These points acted in the model as "sinks" for wildlife trade with different conductance values (number of individuals confiscated) of the resistor tying each ground node to ground.

We constructed a resistance surface of roads, to provide potential wildlife trade pathways between source and sink locations. We focused our spatial model on road networks as primary conduit for the domestic trade of live parrots (13). Domestic aviation security (e.g., routine X-ray cargo scanning) makes the clandestine air transport of bulky and vocal live animals logistically prohibitive (71), while terrestrial corridors remain the primary and most viable conduit for the domestic live bird trade for millennia (28). Based on a road map of Mexico (https://www.naturalearthdata.com/downloads/10m-cultural-vectors/roads), we constructed a raster assigning low resistance values for large roads ("1" = "Freeway" and "Tollway," "2" = "Primary"), higher values for smaller roads ("3" = "Secondary," "4" = "Other Paved," "5" = "Unpaved"), and highest ("100") for areas where none of these road types occur.

In QGIS 3.34 (https://www.qgis.org), we aligned all raster and vector layers by reprojecting them to the same CRS (EPSG:6362) that is ideal for the area of Mexico. Raster layers were rescaled to the same cell size (30 arc sec or around 1 × 1 km). All layers were clipped to the extent of Mexico. Current maps were generated by CIRCUITSCAPE for each species, and then we calculated the sum of current values from all available species. We visualized this composite map with a linear color ramp using equal intervals in QGIS 3.34.

Potential Uncertainty in Data and Modeling Approaches. One source of uncertainty in the landscape modeling was the lack of precision of the confiscation locations. The PROFEPA dataset did not include details about how and where the confiscations occurred. Improved databasing is needed to make collected information even more useful to law enforcement, via analyses like in the present study. One solution to collect more granular data on the wildlife trade is to employ genetic techniques to assign confiscated birds to populations or even individuals. Genetic techniques have been used in wildlife forensic investigations about parrots in a few cases to identify traded species from eggs (72), determining their geographic origin (73) or distinguish captive versus wild birds via parentage analyses (74). Some of these results were even used and accepted in court (72, 75).

The other caveat is that the data were recorded by the regional environmental police offices (PROFEPA), which have autonomy over prioritizing their yearly budget, e.g., into confiscations vs. crime prevention. It is possible that in certain years or states, PROFEPA had a larger budget allowing for greater enforcement and a higher number of confiscations. However, PROFEPA is federally funded and has had its budget reduced since 2010, yet, as we showed, the magnitude of confiscations since that year (until the COVID-19 pandemic) did not drop noticeably as one would expect if there were a strong correlation between available budget and confiscated animals.

Data, Materials, and Software Availability. The R-code used for the analysis and visualizations is available on FigShare (41). Interactive online results are available for vetted law enforcement officers at https://www.stopparrottrade.org (20) after registration. A video of the study is available on the TIB AV-Portal (21).

ACKNOWLEDGMENTS. We thank PROFEPA for collecting and organizing the data and making it available for our research. We thank Stu Butchart and Tom Scott for help and discussion about the Red List Index. We are grateful to the Cornell Lab of Ornithology for the eBird Status data and providing illustrations on parrots. G.O. was funded by Australian Research Council DECRA Fellowship (DE230100085) and the Loro Parque Fundación (PP-250-2024).

Author affiliations: [a]Fenner School of Environment and Society, College of Systems and Society, The Australian National University, Canberra, ACT 2600, Australia; [b]King's Forensics, Department of Analytical, Environmental and Forensic Sciences, Faculty of Life Sciences and Medicine, King's College London, London SE1 9NH, United Kingdom; [c]World Wildlife Fund Mexico, Ciudad de México 03100, Mexico; [d]BirdLife International, Cambridge CB2 3QZ, United Kingdom; and [e]Center for Global Discovery and Conservation Science, Arizona State University, Hilo, HI 96720

1. B. R. Scheffers, B. F. Oliveira, I. Lamb, D. P. Edwards, Global wildlife trade across the tree of life. *Science* **366**, 71–76 (2019).
2. E. C. Holmes *et al.*, The origins of SARS-CoV-2: A critical review. *Cell* **184**, 4848–4856 (2021).
3. INTERPOL, Illegal wildlife trade has become one of the 'world's largest criminal activities (2023). https://www.interpol.int/News-and-Events/News/2023/Illegal-wildlife-trade-has-become-one-of-the-world-s-largest-criminal-activities. Accessed 23 January 2025.
4. A. Hughes *et al.*, Determining the sustainability of legal wildlife trade. *J. Environ. Manage.* **341**, 117987 (2023).
5. G. Olah *et al.*, Ecological and socio-economic factors affecting extinction risk in parrots. *Biodivers. Conserv.* **25**, 205–223 (2016).
6. D. T. C. Chan, E. S. K. Poon, A. T. C. Wong, S. Y. W. Sin, Global trade in parrots–Influential factors of trade and implications for conservation. *Global Ecol. Conserv.* **30**, e01784 (2021).
7. Wild Bird Conservation Act, USA (16 U.S.C. 4901-4916) (1992). https://www.govinfo.gov/content/pkg/USCODE-2017-title16/pdf/USCODE-2017-title16-chap69.pdf. Accessed 6 December 2024.
8. United Mexican States, DECRETO por el que se adiciona un artículo 60 Bis 2 a la Ley General de Vida Silvestre (2008). https://www.animallaw.info/statute/mx-bird-parrot-ban-spanish-decree-which-article-60-2-general-law-wildlife. Accessed 3 August 2026.
9. A. Loza *et al.*, Two-year follow-up of the COVID-19 pandemic in Mexico. *Front. Public Health* **10**, 1050673 (2023).
10. S. H. M. Butchart *et al.*, Measuring trends in extinction risk: A review of two decades of development and application of the Red List Index. *Philos. Trans. R. Soc. Lond. B, Biol. Sci.* **380**, 20230206 (2025).
11. J. F. Brodie *et al.*, Correlation and persistence of hunting and logging impacts on tropical rainforest mammals. *Conserv. Biol.* **29**, 110–121 (2015).
12. D. L. Vergara-Tabares, J. M. Cordier, M. A. Landi, G. Olah, J. Nori, Global trends of habitat destruction and consequences for parrot conservation. *Glob. Change Biol.* **26**, 4251–4262 (2020).
13. P. Romero-Vidal *et al.*, Poaching sources and trade routes in Peru and Ecuador warn of the unsustainable rural demand for preferred parrot species. *Conserv. Sci. Pract.* **5**, e12936 (2023).
14. J. C. Cantú, M. E. Sánchez, M. Grosselet, J. Silva, *The Illegal Parrot Trade in Mexico: A Comprehensive Assessment* (Defenders of Wildlife, 2007).
15. S. Pires, R. V. Clarke, Are parrots CRAVED? An analysis of parrot poaching in Mexico. *J. Res. Crime Delinq.* **49**, 122–146 (2012).
16. J. L. Tella, F. Hiraldo, Illegal and legal parrot trade shows a long-term, cross-cultural preference for the most attractive species increasing their risk of extinction. *PLoS ONE* **9**, e107546 (2014).
17. S. F. Pires, G. Olah, D. Nandika, D. Agustina, R. Heinsohn, What drives the illegal parrot trade? Applying a criminological model to market and seizure data in Indonesia. *Biol. Conserv.* **257**, 109098 (2021).

18. B. H. McRae, B. G. Dickson, T. H. Keitt, V. B. Shah, Using circuit theory to model connectivity in ecology, evolution, and conservation. *Ecology* **89**, 2712–2724 (2008).
19. G. Olah *et al.*, Exploring dispersal barriers using landscape genetic resistance modelling in scarlet macaws of the Peruvian Amazon. *Landsc. Ecol.* **32**, 445–456 (2017).
20. The Australian National University, Forensic toolkit for tracking the illegal parrot trade (2026). https://stopparrottrade.org. Accessed 3 August 2026.
21. G. Olah, R. Léon-Pérez, A. J. Berryman, G. Asner, R. Heinsohn, Video abstract: Shifting drivers and predictable corridors of an illegal wildlife trade network. TIB AV-Portal. https://doi.org/10.5446/73708. Deposited 3 August 2026.
22. D. Brack, Illegal logging and the illegal trade in forest and timber products. *Int. For. Rev.* **5**, 195–198 (2003).
23. G. A. Petrossian, Preventing illegal, unreported and unregulated (IUU) fishing: A situational approach. *Biol. Conserv.* **189**, 39–48 (2015).
24. G. Bichler, A. Malm, T. Cooper, Drug supply networks: A systematic review of the organizational structure of illicit drug trade. *Crime Sci.* **6**, 2 (2017).
25. D. van Uhm, N. South, T. Wyatt, Connections between trades and trafficking in wildlife and drugs. *Trends Organ. Crime* **24**, 425–446 (2021).
26. L. Wagner, D. Siller, R. Landa, *People and Forests at Risk: Organized Crime, Trafficking in Persons and Deforestation in Chihuahua, Mexico* (Global Initiative Against Transnational Organized Crime, 2020).
27. G. Olah, B. T. Smith, L. Joseph, S. C. Banks, R. Heinsohn, Advancing genetic methods in the study of parrot biology and conservation. *Diversity* **13**, 521 (2021).
28. G. Olah *et al.*, Ancient DNA and spatial modeling reveal a pre-Inca trans-Andean parrot trade. *Nat. Commun.* **17**, 2117 (2026).
29. D. Yeo *et al.*, Uncovering the magnitude of African pangolin poaching with extensive nanopore DNA genotyping of seized scales. *Conserv. Biol.* **38**, e14162 (2024).
30. J. M. Capriles *et al.*, Pre-Columbian transregional captive rearing of Amazonian parrots in the Atacama Desert. *Proc. Natl. Acad. Sci. U.S.A.* **118**, e2020020118 (2021).
31. C. W. Schwartz, S. Plog, P. A. Gilman, *Birds of the Sun: Macaws and People in the U.S.* (Southwest and Mexican Northwest University of Arizona Press, 2022).
32. J. A. Cruz, E. Corona-M, E. Gallaga-Murrieta, The preclassic military macaw (*Ara militaris*) from the Cueva de Avendaños (Chihuahua, Mexico) was not locally procured. *Int. J. Osteoarchaeol.* **33**, 642–651 (2023).
33. P. Romero-Vidal, M. Carrete, F. Hiraldo, G. Blanco, J. L. Tella, Confounding rules can hinder conservation: Disparities in law regulation on domestic and international parrot trade within and among neotropical countries. *Animals* **12**, 1244 (2022).
34. S. H. M. Butchart *et al.*, Measuring trends in extinction risk: A review of two decades of development and application of the Red List Index. *Philos. Trans. B* **380**, 20230206 (2025).
35. S. H. M. Butchart *et al.*, Using red list indices to measure progress towards the 2010 target and beyond. *Philos. Trans. R. Soc. B, Biol. Sci.* **360**, 255–268 (2005).
36. S. H. M. Butchart *et al.*, Improvements to the Red List Index. *PLoS ONE* **2**, e140 (2007).
37. A. S. L. Rodrigues *et al.*, Spatially explicit trends in the global conservation status of vertebrates. *PLoS ONE* **9**, e113934 (2014).
38. S. H. M. Butchart *et al.*, Global biodiversity: Indicators of recent declines. *Science* **328**, 1164–1168 (2010).
39. H. Wickham, *ggplot2: Elegant Graphics for Data Analysis* (Springer-Verlag, New York, NY, 2016).
40. T. L. Pedersen, ggraph: An implementation of grammar of graphics for graphs and networks (Version 2.2.2, CRAN, 2024).
41. G. Olah, R. Léon-Pérez, A. J. Berryman, G. Asner, R. Heinsohn, Confiscation dataset and scripts to analyze the Mexican parrot trade (1997–2024). Figshare. https://doi.org/10.6084/m9.figshare.29400944. Deposited 3 August 2026.
42. HBW and BirdLife International, Handbook of the Birds of the World and BirdLife International digital checklist of the birds of the world. Version 10 (2025). https://datazone.birdlife.org/about-our-science/taxonomy#birdlife-s-taxonomic-checklist. Accessed 17 October 2025.
43. F. E. Rheindt *et al.*, Avilist: A unified global bird checklist. *Biodivers. Conserv.* **34**, 3359–3376 (2025).
44. R. V. G. Clarke, *Hot Products: Understanding, Anticipating and Reducing Demand for Stolen Goods (Vol. 112). London: Home Office, Policing and Reducing Crime Unit, Research, Development and Statistics Directorate* (Citeseer, 1999).
45. S. F. Pires, R. V. Clarke, Sequential foraging, itinerant fences and parrot poaching in Bolivia. *Br. J. Criminol.* **51**, 314–335 (2011).
46. J. Fox, S. Weisberg, *An R Companion to Applied Regression, Third Edition* (Sage, 2019).
47. United Mexican States, NORMA Oficial Mexicana NOM-059-ECOL-2001, Protección ambiental - Especies nativas de México de flora y fauna silvestres - Categorías de riesgo y especificaciones para su inclusión, exclusión o cambio - Lista de especies en riesgo (2001). https://www.biodiversidad.gob.mx/pdf/NOM-059-ECOL-2001.pdf. Accessed 3 August 2026.
48. United Mexican States, MODIFICACIÓN del Anexo Normativo III, Lista de especies en riesgo de la Norma Oficial Mexicana NOM-059-SEMARNAT-2010 (2019). https://www.dof.gob.mx/nota_detalle.php?codigo=5578808&fecha=14/11/2019#gsc.tab=0. Accessed 3 August 2026.
49. T. Juniper, M. Parr, *Parrots: A Guide to Parrots of the World* (Yale University Press, 1998).
50. J. M. Forshaw, *Parrots of the World* (CSIRO Publishing, 2011).
51. BirdLife International and Handbook of the Birds of the World, Bird species distribution maps of the world. Version 2022.2 (2022). https://datazone.birdlife.org/species/requestdis. Accessed 6 December 2022.
52. WorldPop and CIESIN, Global High resolution population denominators project (2020). https://doi.org/10.5258/SOTON/WP00675. Deposited 22 June 2020.
53. D. Fink *et al.*, Modeling avian full annual cycle distribution and population trends with citizen science data. *Ecol. Appl.* **30**, e02056 (2020).
54. M. Vall-llosera, P. Cassey, 'Do you come from a land down under?' Characteristics of the international trade in Australian endemic parrots. *Biol. Conserv.* **207**, 38–46 (2017).
55. BirdLife International, IUCN Red List for birds (2025). https://datazone.birdlife.org. Accessed 14 May 2025.
56. G. Olah *et al.*, Parrots of Oceania—A comparative study of extinction risk. *Emu* **118**, 94–112 (2018).
57. T. J. Regan *et al.*, The consistency of extinction risk classification protocols. *Conserv. Biol.* **19**, 1969–1977 (2005).
58. K. Delhey, M. Valcu, C. Muck, J. Dale, B. Kempenaers, Evolutionary predictors of the specific colors of birds. *Proc. Natl. Acad. Sci. U.S.A.* 120, e2217692120 (2023).
59. L. Benedict, A. Charles, A. Brockington, C. R. Dahlin, A survey of vocal mimicry in companion parrots. *Sci. Rep.* **12**, 20271 (2022).
60. R Core Team, *R: A Language and Environment for Statistical Computing* (R Core Team, 2025). Deposited 2025.
61. K. Bartoń, MuMIn: Multi-model inference (Version 1.48.19, CRAN, 2025).
62. W. Jetz *et al.*, Global distribution and conservation of evolutionary distinctness in birds. *Curr. Biol.* **24**, 919–930 (2014).
63. D. L. Rabosky, No substitute for real data: A cautionary note on the use of phylogenies from birth–death polytomy resolvers for downstream comparative analyses. *Evolution* **69**, 3207–3216 (2015).
64. A. Ives *et al.*, phyr: Model based phylogenetic analysis (Version 1.1.3, CRAN, 2020).
65. D. Li, R. Dinnage, L. A. Nell, M. R. Helmus, A. R. Ives, phyr: An R package for phylogenetic species-distribution modelling in ecological communities. *Methods Ecol. Evol.* **11**, 1455–1463 (2020).
66. A. R. Ives, R^2s for correlated data: Phylogenetic models, LMMs, and GLMMs. *Syst. Biol.* **68**, 234–251 (2019).
67. B. F. L. Manly, L. McDonald, D. L. Thomas, T. L. McDonald, W. P. Erickson, *Resource Selection by Animals: Statistical Design and Analysis for Field Studies* (Springer Science & Business Media, 2007).
68. P. Romero-Vidal *et al.*, Opportunistic or non-random wildlife crime? Attractiveness rather than abundance in the wild leads to selective parrot poaching. *Diversity* **12**, 314 (2020).
69. INEGI, Instituto Nacional de Estadística y Geografía: Mexico administrative level 0–2 boundaries (COD-AB) dataset (2024). https://data.humdata.org/dataset/cod-ab-mex. Accessed 6 December 2024.
70. K. R. Hall *et al.*, Circuitscape in Julia: Empowering dynamic approaches to connectivity assessment. *Land* **10**, 301 (2021).
71. A. D. Setiyani, M. A. Ahmadi, An overview of illegal parrot trade in Maluku and North Maluku provinces. *For. Soc.* **4**, 48–60 (2020).
72. M. L. Coghlan *et al.*, Egg forensics: An appraisal of DNA sequencing to assist in species identification of illegally smuggled eggs. *Forensic Sci. Int. Genet.* **6**, 268–273 (2012).
73. F. A. Rivera-Ortíz, J. Juan-Espinosa, S. Solórzano, A. M. Contreras-González, M. del C. Arizmendi, Genetic assignment tests to identify the probable geographic origin of a captive specimen of military macaw (*Ara militaris*) in Mexico: Implications for conservation. *Diversity* **13**, 245 (2021).
74. W. G. Coetzer, C. T. Downs, M. R. Perrin, S. Willows-Munro, Testing of microsatellite multiplexes for individual identification of Cape Parrots (*Poicephalus robustus*): Paternity testing and monitoring trade. *PeerJ* **5**, e2900 (2017).
75. N. E. White *et al.*, Application of STR markers in wildlife forensic casework involving Australian black-cockatoos (*Calyptorhynchus* spp.). *Forensic Sci. Int. Genet.* **6**, 664–670 (2012).